Scientific Research Publishing

Open Journal of Social Sciences, 2026, 14(3), 668-687
https://www.scirp.org/journal/jss
ISSN Online: 2327-5960
ISSN Print: 2327-5952

Dynamic Correlation between Implied Volatility Spreads and Movement of CSI 300 ETF: Regime Identification

Han Yang[1*], Yintao Hu[2*], Zhijing Wang[2], Naixue Xiong[3], Rui Liang[2#], Jerome Yen[2#]

[1]Institute of Collaborative Innovation, University of Macau, Macau, China
[2]Faculty of Science and Technology, University of Macau, Macau, China
[3]School of Computer Science and Engineering, Hunan University of Science and Technology (HUST), Xiangtan, China
Email: mc46530@um.edu.mo, mc45123@um.edu.mo, mc55210@um.edu.mo, xiongnaixue@gmail.com, [#]yc27977@um.edu.mo, [#]jeromeyen@um.edu.mo

How to cite this paper: Yang, H., Hu, Y. T., Wang, Z. J., Xiong, N. X., Liang, R., & Yen, J. (2026). Dynamic Correlation between Implied Volatility Spreads and Movement of CSI 300 ETF: Regime Identification. *Open Journal of Social Sciences, 14,* 668-687.
https://doi.org/10.4236/jss.2026.143037

Received: February 9, 2026
Accepted: March 28, 2026
Published: March 31, 2026

Abstract

Implied volatility (IV) is crucial for gauging market risk and potential price movements, as exemplified by volatility indices such as VIX for the S&P 500. However, China's A-share markets exhibit unique volatility dynamics due to their distinctive investor composition, T + 1 settlement rules, and limited short-selling instruments. This study constructs an IV Spread indicator—the difference between put and call implied volatilities—to capture the dynamic relationship between IV movements and CSI 300 ETF price changes. Using the Black-Scholes model, we calculate IV and synthesize cross-maturity spread components. We then employ dynamic correlation analysis to examine the relationship between IV Spread changes and underlying asset prices. To identify market sentiment pivot points and extreme market conditions, we apply a two-stage change-point detection method: first merging segments via the Bottom-Up algorithm, then selecting optimal segments using Lavielle's Maximum Curvature Criterion. This approach identifies 18 stable macro-states with significant transitions between them. Our findings demonstrate that IV Spread and its derivatives effectively identify regime switching and extreme market conditions. Furthermore, we incorporate unstructured data to validate market sentiment shifts, examining events surrounding major correlation breakpoints and price pivot points. This multi-modal approach provides insights for future research on asset movement prediction.

*Co-first authors.
[#]Corresponding authors.

Keywords

Implied Volatility Spread, Regime Switching, Multi-Modal Data, A-Share Market

1. Introduction

The use of derivatives to predict future asset movements has been a central research topic since their introduction to financial markets (Ross, 1976; Beckers, 1981). Among these instruments, implied volatility (IV) serves as a critical factor in pricing options and structured products, while simultaneously reflecting investor perceptions of market dynamics and hedging behaviors, such as purchasing put options to mitigate downside risks.

The predictive power of volatility indices is well-documented. For instance, the VIX, introduced by the Chicago Board Options Exchange in 1993 (CBOE, 1993), maintains a stable negative correlation of approximately -0.75 with the S&P 500 index. However, this relationship exhibits instability under certain market conditions. During the COVID-19 outbreak in March 2020, the VIX averaged 57.74, peaking at 82.69 on March 16, indicating heightened demand for downside protection. Yet, in other scenarios—such as when investors utilize put options to lock in profits during market uptrends, the expected negative correlation may reverse. This instability motivates our investigation into alternative indicators capable of enhancing prediction accuracy and identifying the limitations of existing models.

Accordingly, we propose the IV Spread, defined as the difference between put and call implied volatilities, along with its moving average (MA), as novel indicators for capturing market sentiment dynamics. This study examines whether the IV Spread provides superior correlation with underlying asset movements compared to individual put or call IVs and identifies the specific regimes where this indicator most effectively signals necessary trading strategy adjustments. Additionally, we explore whether incorporating unstructured data, such as news sentiment, can strengthen confidence in generated trading signals. Given the distinct volatility dynamics of emerging markets compared to mature ones, the Chinese A-share market, with its unique microstructure, provides an ideal setting to test the effectiveness of the proposed IV Spread indicator.

The Chinese A-share market presents a unique testing environment for this framework. Unlike mature markets where the VIX methodology predominates, China's volatility dynamics exhibit distinct characteristics: call IV frequently exceeds put IV—a phenomenon rarely observed in mature markets such as the U.S. and Hong Kong SAR. Furthermore, market microstructure features, including T + 1 settlement rules, retail investor dominance, and limited short-selling mechanisms, contribute to pronounced volatility asymmetries. We selected the CSI 300 ETF as our test asset to evaluate the proposed indicators within this context.

To calculate IV, we employ the Black-Scholes model (Black & Scholes, 1973) solved via numerical methods (Brent and Bisection algorithms; Press et al., 1992).

While alternative approaches exist—such as stochastic volatility models (Heston, 1993; Hagan et al., 2002) or local volatility frameworks (Dupire, 1994)—our focus on IV Spread dynamics means that the specific IV calculation method is less critical than the spread construction itself, as long as the IV estimation is sufficiently accurate. Our findings demonstrate that neither put IV nor call IV alone captures complete market information. The IV Spread, particularly when smoothed via moving averages and augmented with higher-order derivatives, provides richer insights into investor expectations, risk appetite shifts, and structural market changes. This framework enables more precise identification of momentum phases, extreme market conditions, and potential pivot points.

The remainder of this paper is organized as follows. Section 2 reviews related literature and theoretical foundations. Section 3 details the methodology and data. Section 4 presents empirical results. Section 5 concludes for future research.

2. Related Work

2.1. Implied Volatility

Implied volatility (IV) represents the market's expectation of future volatility derived from inverting option pricing models. The Black-Scholes model (Black & Scholes, 1973) established the foundational relationship between option prices and underlying asset volatility, assuming geometric Brownian motion and constant volatility. Within this framework, IV equates theoretical prices with observed market prices, functioning as a bridge between pricing theory and market practice.

Computationally, IV requires the underlying asset price, strike price, risk-free rate, time to expiration, option market price, and option type as inputs. Numerical methods such as the Newton-Raphson algorithm solve for the volatility parameter satisfying the pricing equation. As a forward-looking indicator, IV encapsulates investor expectations regarding future risk (Black & Scholes, 1973), motivating continuous refinement of calculation methodologies (Andersen et al., 2003; Bollerslev & Zhou, 2002; Bollerslev et al., 2009).

Despite extensive research on IV estimation, relatively few studies examine IV Spreads' explanatory power regarding market behavior and predictive capacity for asset price movements. A notable limitation of the Black-Scholes framework is its inability to explain the empirically observed "volatility smile," wherein IV varies asymmetrically across strike prices. To address this deficiency, scholars have developed extended models, including deterministic volatility surfaces (Derman & Kani, 1994; Derman, Kani, & Chriss, 1996; Dupire, 1994; Rubinstein, 1994). However, these approaches remain inadequate in capturing the dynamic characteristics and time-varying intensity of IV-asset price correlations. These limitations have catalyzed the development of stochastic volatility models and motivated our focus on IV Spreads, which better reflect market sentiment dynamics than individual IVs.

2.2. Volatility and Market Dynamics

While volatility indices such as the CBOE VIX have been extensively employed in

U.S. markets, IV Spread dynamics exhibit substantial cross-market heterogeneity driven by distinct investor compositions and regulatory frameworks.

For the Hong Kong SAR Market, in Hang Seng Index (HSI) derivatives, IV Spreads demonstrate stable structural characteristics, with put IV consistently exceeding call IV. For the Hong Kong SAR Market, in Hang Seng Index (HSI) derivatives, IV Spreads demonstrate stable structural characteristics, with put IV consistently exceeding call IV. This persistent skew reflects institutional demand for downside protection, particularly from asset managers and insurance firms engaged in sustained hedging activities (Hull & White, 1987; Bollen & Whaley, 2004; Fung et al., 2024). The VHSI index, constructed primarily from short-term put options, institutionalizes this asymmetry as a market fear barometer. Furthermore, Lin and Lu (2015) demonstrate that IV changes surrounding forecasted pivot points and rating adjustments correlate significantly with future price movements, particularly under high information asymmetry. This suggests that IV Spreads capture informed trading behavior and hedging demand beyond raw volatility measures. Nevertheless, Chen and Lai (2013) note that VHSI-HSI correlations exhibit time-varying and asymmetric features, with investors particularly sensitive to negative returns, indicating that these spreads remain sensitive to market sentiment shifts and macroeconomic conditions.

For the A-Share Market, in contrast, China's A-share market exhibits markedly different IV Spread dynamics due to its retail-dominated investor base and distinct microstructural features. Retail investors' sentiment-driven, momentum-chasing behavior often inflates call IV beyond put IV during bullish periods, despite persistent downside risks (Blitz et al., 2021). Limited hedging demand among unsophisticated participants further suppresses put IV, reversing the typical skew observed in institutional markets. Information asymmetry compounds these effects: domestic institutions leverage superior information access through local networks and regulatory familiarity, enabling anticipatory trading that distorts option pricing dynamics (Chan et al., 2008). Consequently, call options frequently serve as vehicles for directional speculation rather than downside protection. Recent empirical evidence confirms these patterns—Zhang and Zi (2025), analyzing 50ETF options on the Shanghai Stock Exchange, document that A-share IV Spreads possess significant return predictability while remaining highly sensitive to market structure, investor composition, and regulatory design.

2.3. IV Spreads and Market Sentiment

Zhang and Xiang (2008) introduced moneyness—defined as the logarithmic ratio of strike price to forward price—to construct parametric implied volatility smirk curves. Their findings indicate that out-of-the-money puts exhibit significantly higher implied volatility than at-the-money contracts, reflecting market pricing of downside tail risk. This negative skew is consistently observed in equity index options, where the steepness of the smirk forecasts lower subsequent market returns, consistent with investors pricing crash risk into downside options (Xing, Zhang,

& Zhao, 2010).

Extending this approach, Johnson (2017) demonstrates that the slope of the VIX term structure predicts variance risk premia across all maturities, with upward-sloping curves associated with larger risk premia and inverted curves signaling diminished or even negative premia. These structural features explain regime-dependent variation in option returns, as the term structure aggregates market expectations about future volatility dynamics.

Put-Call IV Spread Measurement. The IV Spread is conventionally calculated as the difference between put and call IV at identical strike prices and expiration dates. Positive spreads indicate elevated put IV relative to calls, typically reflecting downside protection demand or market fear. Conversely, negative spreads—relatively rare phenomena—suggest call IV exceeds put IV, potentially signaling speculative behavior, liquidity asymmetries, or market inefficiencies. Doran et al. (2013) demonstrate that IV spreads contain information about both firm fundamentals and option mispricing, showing that spreads are positively related to future underlying stock returns but negatively related to future out-of-the-money call option returns due to differential trading behavior between sophisticated and retail investors.

Behavioral and Real-Time Dimensions. Beyond structural modeling, recent research emphasizes behavioral and high-frequency aspects of IV dynamics. Smales (2014) documents dynamic news sentiment effects on implied volatility and stock returns, while Guo et al. (2023) highlight latency-accuracy trade-offs in IV-based trading systems. These findings suggest real-time IV fluctuations significantly influence trading decisions and may contribute to anomalies such as negative IV spreads—a phenomenon frequently observed in the A-share market due to its retail-dominated structure (see Section2.2). From a portfolio management perspective, DeMiguel et al. (2013) demonstrate that incorporating option-implied volatility and skewness enhances risk assessment and improves portfolio performance. Yue et al. (2020) further examine volatility smile dynamics in Chinese equity options, revealing how market structure and investor composition shape IV curves.

Predictive Power and Volatility Premium. The predictive efficacy of IV has been validated. Beckers (1981) and Andersen et al. (2003) establish that IV consistently outperforms historical volatility in forecasting short-term price movements. However, the well-documented volatility premium—wherein IV systematically exceeds realized volatility—suggests markets incorporate compensation for tail risk and uncertainty. This premium may distort expected put-call IV relationships, as documented by Bakshi and Kapadia (2003), Whaley (2000), and Goyal and Saretto (2009).

2.4. Lingering Effects of the COVID-19 Natural Experiment

The COVID-19 pandemic generated an unprecedented structural break in Chinese financial markets. During Q1-2020, foreign investors exhibited stronger negative trading behaviors compared to the pre-COVID-19 period, reflecting height-

ened market uncertainty and information asymmetry (Bing & Ma, 2021). This period saw significant disruptions in the ETF-option markets, where the at-the-money put-minus-call implied volatility spread on the 50 ETF remained negative for 61 consecutive trading days, averaging −1.8 percentage points and reaching a nadir of −3.1 percentage points—a stark contrast to the consistently positive spreads observed during 2016-2019. This inversion did not reflect diminished downside hedging demand; rather, city-lockdown headlines triggered a retail surge into call options to speculate on policy bailouts, while institutional hedging activity simultaneously collapsed. The resulting demand imbalance elevated call IV above put IV for a prolonged period.

Following the zero-COVID policy exit in late 2022, turnover normalized, yet behavioral patterns persisted. The 2023 SSE Fact-Book indicates individual investors accounted for 76% of trading volumes, 4 percentage points below 2021 levels. Zhang and Zi (2025) document that negative-spread days constituted 18% of the 2023 calendar year, compared with 7% in the pre-pandemic seven-year average. These negative prints cluster predominantly in the 10:00-10:30 window, coinciding with peak retail order flow, confirming that sentiment-driven directional imbalances have become a durable market microstructure feature.

The price-discovery channel exhibits similar persistence. Du et al. (2022) demonstrate that institutional net buying strengthens momentum in high-priced stocks where retail participation is constrained, while retail-driven noise trading attenuates price trends, with this pattern persisting through the pandemic period. Zhang and Zi (2025) further note that short-term momentum effects in Chinese markets are masked by noise trading, with institutional participation strengthening momentum persistence, particularly in periods of heightened information asymmetry.

Given that the period 23 January 2020-31 December 2022 contains persistent negative spreads, extreme retail noise, and exogenous policy shocks, we exclude it entirely and anchor our empirical window to the post-COVID period 1 January 2023-31 March 2025. This 27-month interval is sufficiently long to capture diverse market regimes, avoids tail events that would bias parameter estimates, and retains the essential microstructural feature—frequent negative spreads—enabling out-of-sample verification of the IV-spread framework. This sample selection enhances both the robustness and credibility of our findings.

3. Methodology

3.1. The Proposed Framework

This section presents the procedure for utilizing CSI 300 ETF option data to identify regimes. The framework comprises three stages: input data preprocessing, parameter calibration, and regime identification, as illustrated in **Figure 1**.

The empirical implementation requires efficient calculation of IVs, IV Spreads, and their dynamic correlations with underlying asset movements. As established in preceding sections, IV Spread serves as the primary predictive input. We subsequently construct a regime identification framework that analyzes correlation strength and

directional dynamics between IV Spread changes and asset price movements, enabling systematic generation of trading signals across distinct market states.

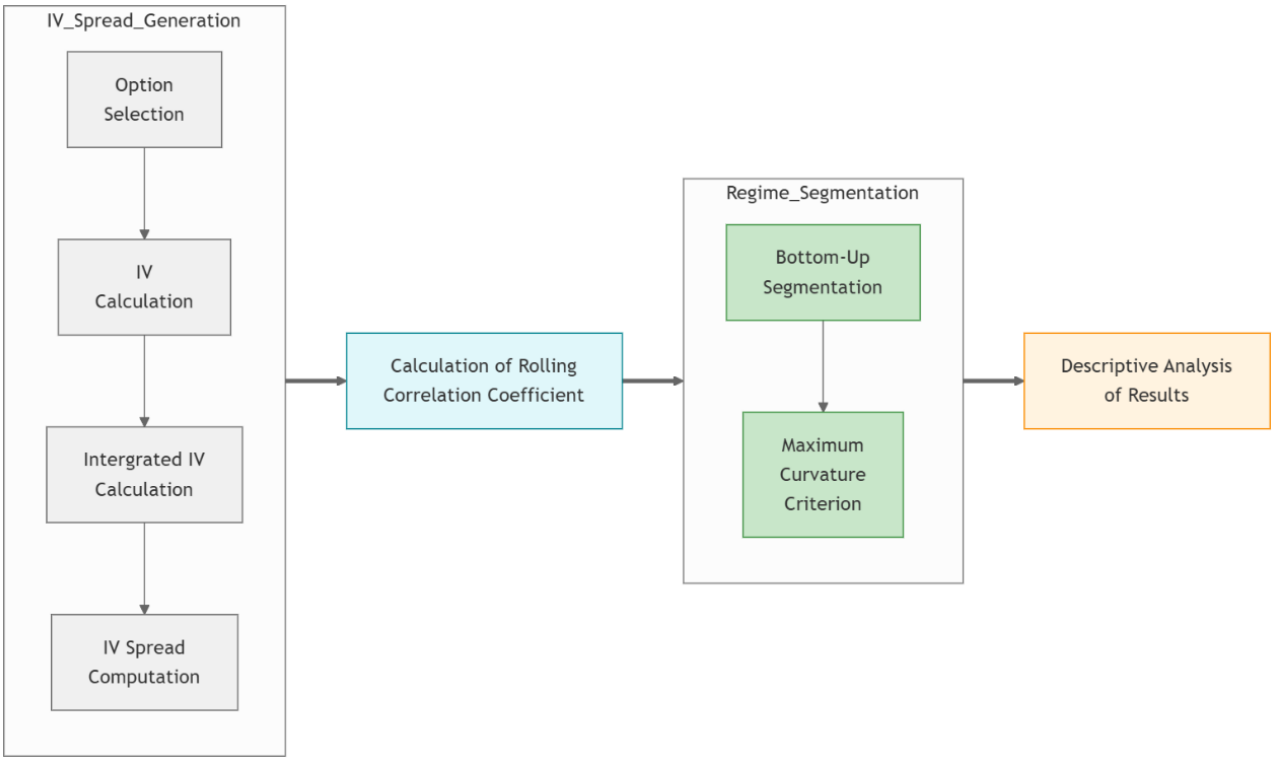

Figure 1. Framework of regime segmentation.

3.2. Options Data Preprocessing

3.2.1. IV Calculation

The Options data contains a wide range of contracts with different strike prices and time to maturity. We choose the most well-known Black-Scholes (BS) model to calculate the implied volatility. And Implied Volatility (IV) is a parameter component of the B-S model. The Black-Scholes formula for call options and put options is as follows:

$$P_c = N(d_1)S_0 - N(d_2)Ke^{-rt}. \quad (1)$$

$$P_p = N(-d_2)Ke^{-rt} - N(-d_1)S_0. \quad (2)$$

where P_c is the price of a call option, P_p is the price of a put option, S_0 is the underlying asset price, K is the strike price, r is the risk-free interest rate, t is the time to maturity.

To calculate the IV, we take the market price of the option (P_{mkt}), entering it into the Black-Scholes formula, and back-solving for the value of the volatility. There are various numerical approaches to calculating implied volatility, such as Brent, Newton-Raphson, Secant Methods, etc.

3.2.2. Generate IV Spread

IV Spread is the Spread between the IV for the call option (IVC) and for the put

option (IVP), which is also significantly related to future market returns. The market will rapidly (slowly) go up when the IV Spread increases (decreases) when the IVC is larger than the IVP. While IVC is smaller than IVP, the market will rapidly (slowly) go down with the increment (decrement) of the Spread. Hence, we choose the IV Spread as a new predictor since it contains information about the trend of the CSI 300 ETF. We construct the measurement of the average IV Spread information using the historical data. Specifically, at each point, the average IV Spread is obtained as the cross-sectional average of the differences between IVC and IVP. The following steps demonstrate the calculation process of IV Spread.

Step 1: Option Selection Based on Moneyness

For each expiry tenor i, we define two sets of selected options:

1) For Call Options: We select all call options whose strike prices $X_j^{(i)}$ satisfy

$$S_t \le X_j^{(i)} \le S_t \times 1.2$$

Let $C_i = \{j \mid X_j^{(i)} \in [S_t, S_t \times 1.2]\}$ denote the set of indices for selected call options at tenor i. The number of selected call options is $m_i^{(c)} = |C_i|$.

2) For Put Options: We select all put options whose strike prices $X_j^{(i)}$ satisfy

$$S_t \times 0.8 \le X_j^{(i)} \le S_t$$

Let $P_i = \{j \mid X_j^{(i)} \in [S_t \times 0.8, S_t]\}$ denote the set of indices for selected put options at tenor i. The number of selected put options is $m_i^{(p)} = |P_i|$.

Here, $i \in \{1,2,3,4,5,6\}$ is the index for the expiry tenor, j is the index for individual options within tenor i, $X_j^{(i)}$ is the strike price of the j-th option at tenor i, S_t is the underlying asset price at time t.

Step 2: Calculate Implied Volatility for Selected Options

For each selected option (i, j), we use its observed market quotation price $V_{t,j}^{(i)}$ to calibrate its implied volatility using the Black-Scholes model. If the option is a call (i.e., $j \in C_i$), its implied volatility is denoted by $IVC_j^{(i)}$. If the option is a put (i.e., $j \in P_i$), its implied volatility is denoted by $IVP_j^{(i)}$. Specifically, $IVC_j^{(i)}$ and $IVP_j^{(i)}$ are the unique values of σ that satisfy the following equations, respectively:

$$BS_{call}\left(S_t, X_j^{(i)}, T_i, r_t, IVC_j^{(i)}\right) = V_{t,j}^{(i)}$$

$$BS_{put}\left(S_t, X_j^{(i)}, T_i, r_t, IVP_j^{(i)}\right) = V_{t,j}^{(i)}$$

where $BS_{call}(\cdot)$ and $BS_{put}(\cdot)$ denote the Black-Scholes pricing functions for call and put options, respectively. This calibration is performed numerically using methods such as Newton-Raphson or Bisection.

Step 3: Calculate Integrated Implied Volatility

We then compute the integrated IV for call and put options at each tenor i:

1) Integrated IV for Call Options:

$$IVC_{teg}^{(i)} = \frac{1}{m_i^{(c)}} \sum_{j \in c_i} IVC_j^{(i)}. \tag{3}$$

2) Integrated IV for Put Options:

$$IVP_{teg}^{(i)} = \frac{1}{m_i^{(p)}} \sum_{j \in P_i} IVP_j^{(i)} . \quad (4)$$

These integrated values represent smoothed, cross-sectional estimates of the IV surface for calls and puts at each maturity.

Step 4: Define and Compute the IV Spread

Based on the above, we define the IV Spread for each tenor i as the difference between the integrated IV of put options and call options:

$$\xi^{(i)} = IVP_{teg}^{(i)} - IVC_{teg}^{(i)} . \quad (5)$$

Finally, we construct our primary predictive indicator, the Integrated IV Spread, denoted by ξ_{teg}, by taking a weighted average of the spreads across all expiry tenors:

$$\xi_{teg} = \sum_{i=1}^{n} w_i \cdot \xi^{(i)} . \quad (6)$$

where w_i is the weight assigned to tenor i. These weights can be chosen flexibly (e.g., equal weights, liquidity-based weights, or volume-based weights) depending on the application. n is the total number of expiry tenors considered (e.g., $n = 6$).

After careful consideration and testing, we selected weights based on trading volume and maturity date to reflect market activity and term structure dynamics.

This approach mirrors the logic of aggregating signals across dimensions in technical analysis, but here applied across the volatility term structure to produce a consolidated, robust measure of market skew and arbitrage opportunity for strategy design or risk monitoring.

3.2.3. Variable Selection

The sample period covered in our analysis ranged from January 2023 to March 2025 (27 months). We did not include data before January 2023 because the Chinese stock market was significantly affected by COVID-19, which caused significant changes in market structure and investor sentiment due to, for example, lockdowns.

Since the Spreads of the IVs of put contracts and call contracts will be the most important indicator to calculate. As mentioned before, Black Scholes Model was selected to calculate the IV of each option contract. For simplicity, the call options with Strike K between 100% and 120% of the ATM price, as well as the put options with Strike K between 80% to 100% of the ATM price, were selected to calculate the weighted average IVs, and their difference was the IV Spread. The reason that options outside such a range were not selected was due to the scarcity of such deep OTM contracts.

3.3. Calculation of Rolling Correlation Coefficient

Let $\{S_t\}_{t=1}^{T}$ and $\{\xi_t\}_{t=1}^{T}$ denote the time series of the underlying asset price and the custom spread metric, respectively, over a sample period of T trading days.

For a fixed window length w (e.g., $w = 5$ trading days), the rolling sample

correlation coefficient at day t (for $t = w, w+1, ..., n$) is defined as

$$\rho_t = \frac{\sum_{i=t-w+1}^{t}(S_i - \bar{S}_t)(\xi_i - \bar{\xi}_t)}{\sqrt{\sum_{i=t-w+1}^{t}(S_i - \bar{S}_t)^2} \cdot \sqrt{\sum_{i=t-w+1}^{t}(\xi_i - \bar{\xi}_t)^2}}. \quad (7)$$

where $\bar{S}_t = \frac{1}{w}\sum_{i=t-w+1}^{t} S_i$ and $\bar{\xi}_t = \frac{1}{w}\sum_{i=t-w+1}^{t} \xi_i$ are the sample means over the rolling window?

The sequence $\{\rho_t\}_{t=w}^{T}$ constitutes a rolling correlation time series of length $n = T - w + 1$. For convenience, we collect these values into a vector:

$$\boldsymbol{\rho} \triangleq (\rho_w, \rho_{w+1}, ..., \rho_T)' \in \mathbb{R}^n.$$

This vector $\boldsymbol{\rho}$ captures the dynamic dependence structure between S_t and ξ_t over time, and will serve as the primary input for subsequent regime analysis.

3.4. Regime Segmentation in Rolling Correlation Coefficient Time Series

To identify distinct market states, we apply a change-point detection algorithm to the rolling correlation time series $\boldsymbol{\rho}$ defined in Section 3.3.

Specifically, we assume that $\boldsymbol{\rho}$ is piecewise stationary, and seek a partition of its index set $\{1, 2, ..., n\}$ into K contiguous, non-overlapping segments, termed macroscopic state intervals, such that the mean of the correlation coefficients remains relatively stable within each segment, while significant shifts occur between adjacent segments. Within each interval, the meaning of the correlation coefficients remains relatively stable, while significant mean shifts occur between adjacent intervals. Consequently, this problem can be formalized as a multiple change-point detection task (Aminikhanghahi & Cook, 2017).

Let the sequence of state transition points be denoted by $\tau = (\tau_0, \tau_1, ..., \tau_K)$, satisfying

$$\tau_0 = 0 < \tau_1 < \cdots < \tau_K = n$$

The data within the k^{th} regime interval are denoted by $\rho_{\tau_{k-1}+1:\tau_k}$.

We adopt a penalized contrast function (Lavielle, 2005) as the optimization criterion to automatically balance model fit and complexity:

$$\min_{\tau} H(\tau) = J(\tau) + \beta K. \quad (8)$$

where, K denotes the number of macroscopic state intervals, β is the penalty parameter, and $\beta > 0$. $J(K)$ represents the within-segment sum of squared errors (SSE), quantifying the goodness-of-fit of the model to the data. Its computation is given by

$$J(K) = \sum_{k=1}^{K}\sum_{t=\tau_{k-1}+1}^{\tau_k}(\rho_t - \bar{\rho}_{\tau_{k-1}+1:\tau_k})^2. \quad (9)$$

In this study, we adopt the Maximum Curvature Criterion (MCC) proposed by Lavielle (2005) to automatically determine the optimal K. This method implicitly identifies an optimal β, achieving an optimal trade-off between model fit and complexity in the final estimated model.

To solve this optimization problem, we first fix K, and compute the optimal segmentation. Then we employ a data-driven approach to automatically select the optimal value of K. The algorithms are as follows.

1) Bottom-Up Segmentation: For the given K, we employ the Bottom-Up merging strategy (Keogh et al., 2001), that initiates with the finest possible segmentation (each initial segment containing exactly two data points) and iteratively merges the pair of adjacent segments that yields the minimal increase in the sum of squared errors (SSE), continuing until exactly K segments remain. Although this greedy approach does not guarantee a globally optimal solution, it is computationally efficient and well-suited for sequences of moderate scale.

2) Maximum Curvature Criterion: We adopt the MCC proposed by Lavielle (2005). This criterion identifies the elbow point in the normalized SSE curve $\tilde{J}(K)$ by detecting the structural transition in the rate of decline. The point where the second-order difference (discrete curvature) of the curve undergoes a significant change. Define the normalized error as

$$\tilde{J}(K) = \frac{J(K) - J(K_{\max})}{J(1) - J(K_{\max})} \cdot (K_{\max} - 1) + 1. \tag{10}$$

where $K = 1, 2, \ldots, K_{\max}$, and $K_{\max} = \min\left\{20, \left\lfloor \frac{n}{30} \right\rfloor\right\}$ which is the constraint ensuring that each macroscopic state interval contains at least 30 trading days. And the discrete curvature is

$$D(K) = \tilde{J}(K-1) - 2\tilde{J}(K) + \tilde{J}(K+1). \tag{11}$$

The optimal number of states $\hat{K}$ is defined as the largest value of K for which $D(K) > 0.75$.

After segmentation, we will use two indicators to conduct descriptive analysis on the macro regime intervals divided by above algorithms.

1) Period Average of Rolling Correlation Coefficient Series (μ_k): This indicator reflects the average level of linkage between IV Spread and asset prices during the period.

2) Z-Score (z_k): This indicator is used to measure the degree of deviation of the correlation between the interval and the historical norm, and its computation is given by

$$z_k = \frac{\mu_k - \mu}{\sigma}. \tag{12}$$

where μ and σ respectively represent the mean and standard deviation of the rolling correlation coefficient over the entire sample period. Based on Z-score, we can qualitatively describe an interval as "significantly above mean", "significantly below mean", or "within normal fluctuation range".

4. Experimental Results and Descriptive Analysis

4.1. Indicators for Descriptive Analysis of Macro Regime Intervals

Empirical analysis under the Maximum Curvature Criterion ($D(K) > 0.75$) iden-

tifies 18 as the optimal number of regimes ($K = 18$). **Figure 2** presents the sum of squared errors (SSE) and curvature function for optimal K selection, illustrating the trade-off between model fit and parsimony.

The rolling correlation coefficient series is partitioned into 18 contiguous, nonoverlapping intervals (**Figure 3**). Within each segment, correlation coefficients exhibit relative stationarity, while statistically significant mean shifts occur between adjacent intervals.

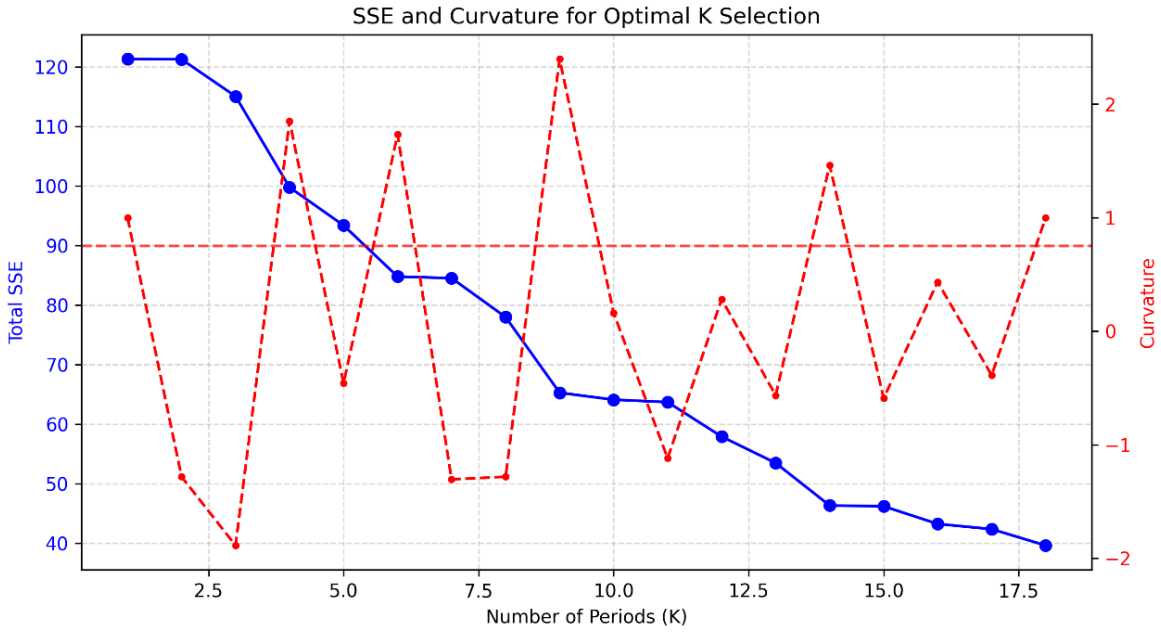

Figure 2. SSE and curvature for optimal k selection.

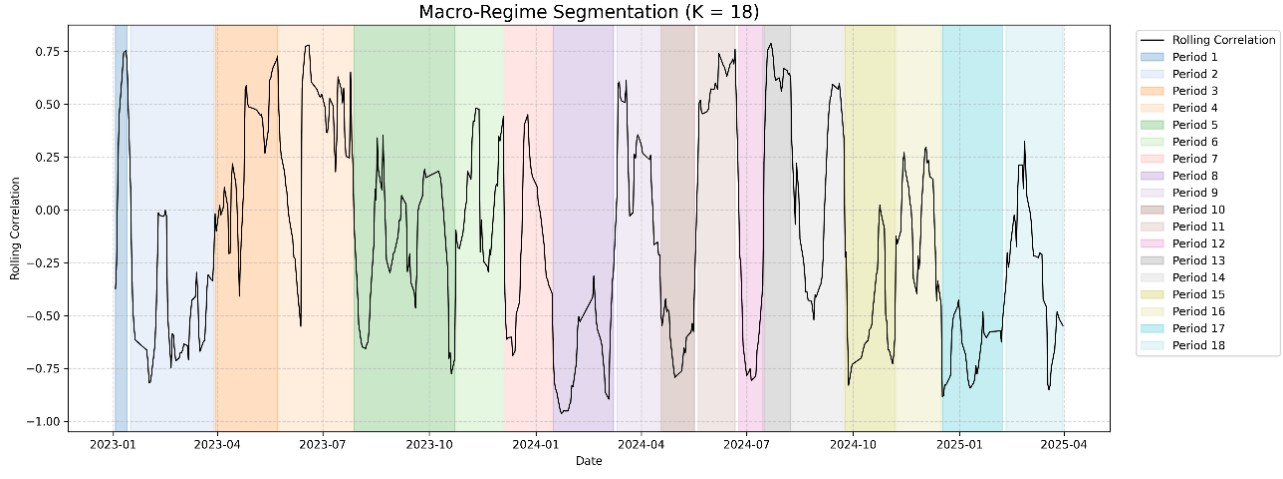

Figure 3. Macro-regime segmentation results.

Table 1 reports the descriptive statistics for these 18 regime intervals. Mean correlation coefficients (μ_k) range from −0.703 to 0.622, with corresponding Z-scores spanning −1.217 to 1.578. This confirms pronounced time-varying structural characteristics in the co-movement between IV Spread and CSI 300 ETF re-

turns. Period 13 (16 July-8 August 2024) exhibits the strongest positive correlation ($\mu = 0.622$, $z = 1.578$), whereas Period 8 (16 January-8 March 2024) displays the most pronounced negative correlation ($\mu = -0.703$, $z = -1.217$).

Table 1. Data summary of macro-regime segmentation results.

Period	Start Date	End Date	Duration (Days)	Mean Correlation	Z-Score
1	2023-01-03	2023-01-13	9	0.400	1.109
2	2023-01-16	2023-03-29	48	−0.474	−0.735
3	2023-03-30	2023-05-23	35	0.252	0.797
4	2023-05-24	2023-07-27	45	0.331	0.964
5	2023-07-28	2023-10-23	56	−0.191	−0.139
6	2023-10-24	2023-12-04	30	0.048	0.365
7	2023-12-05	2024-01-15	29	−0197	−0.150
8	2024-01-16	2024-03-08	33	−0.703	−1.217
9	2024-03-11	2024-04-17	26	0.224	0.738
10	2024-04-18	2024-05-17	19	−0.583	−0.964
11	2024-05-20	2024-06-21	24	0.580	1.490
12	2024-06-24	2024-07-15	16	−0.570	−0.937
13	2024-07-16	2024-08-08	18	0.622	1.578
14	2024-08-09	2024-09-23	30	−0.005	0.254
15	2024-09-24	2024-11-06	27	−0.484	−0.757
16	2024-11-07	2024-12-16	28	0.038	0.186
17	2024-12-17	2025-02-03	32	−0.675	−1.160
18	2025-02-10	2025-03-31	36	−0.257	−0.277

Although most intervals satisfy the conventional 30-day minimum, several shorter regimes (e.g., Periods 10, 12, 13) are retained due to algorithmic sensitivity to local structural breaks. The alternating pattern of positive and negative correlation states reflects frequent regime switching throughout the sample period.

Figure 4 plots mean correlations by regime and their deviation from the historical average (Z-score). The market exhibits no single stable state; rather, it transitions frequently among positive correlation (e.g., Period 13), negative correlation (e.g., Period 8), and neutral phases. These structural breaks confirm that the IV Spread-price relationship functions as a risk-sentiment proxy, with its sign driven by macro-policy expectations and liquidity conditions.

Figure 5 presents within-regime distributions of rolling correlations. Extreme states (e.g., Period 10) display narrow interquartile ranges, indicating highly concentrated and stable correlations—evidence that the segmentation algorithm captures genuine homogeneity. Conversely, neutral regimes (e.g., Period 14) exhibit wide dispersion, implying more chaotic, directionless market behavior.

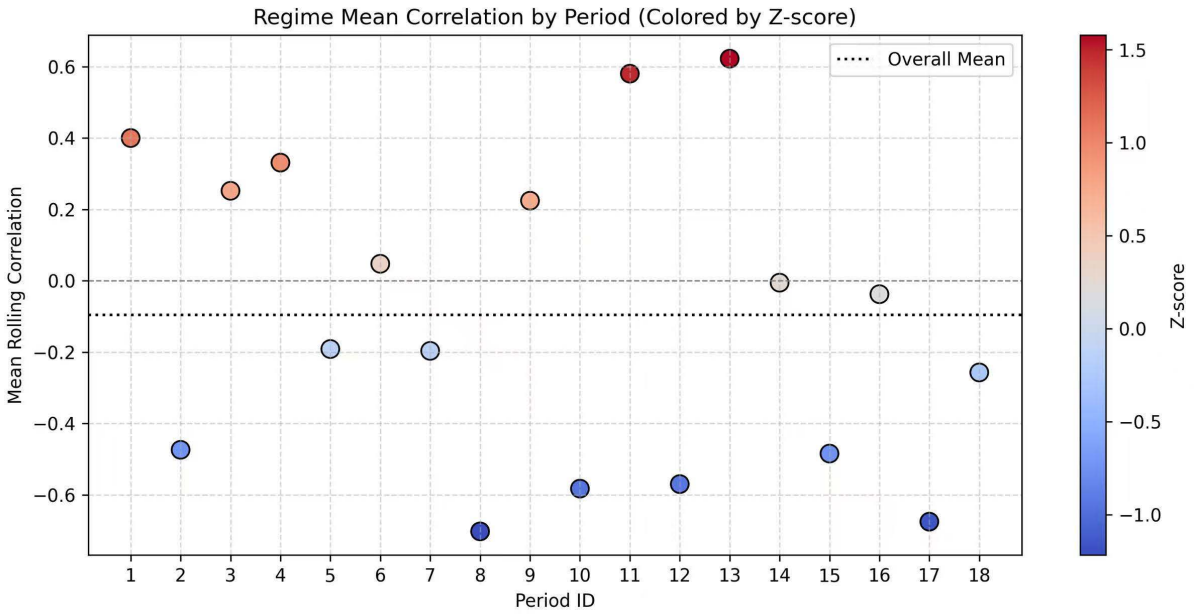

Figure 4. Regime mean correlation by period (Colored by Z-score).

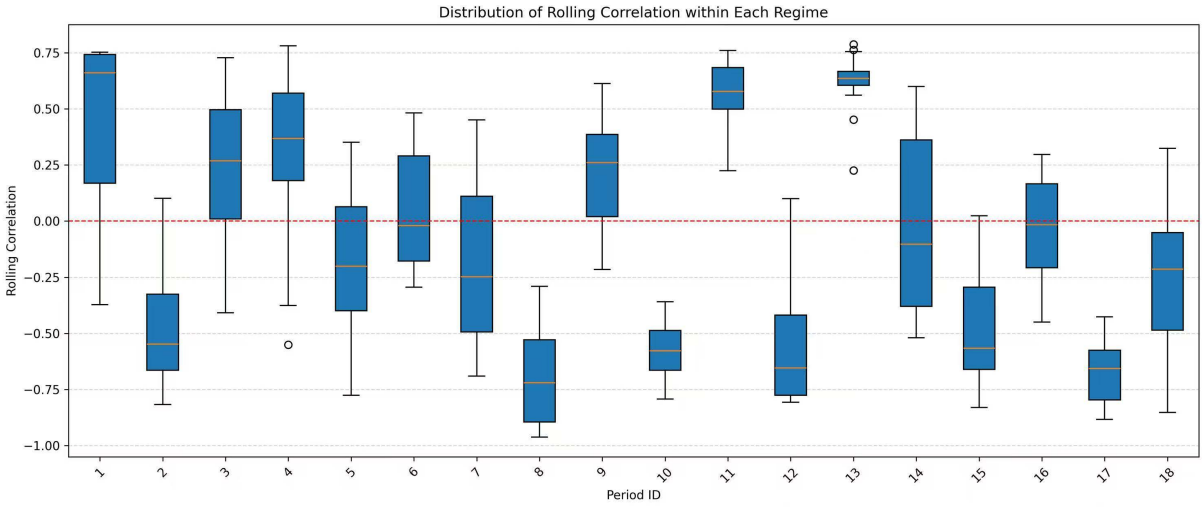

Figure 5. Distribution of rolling correlation within each regime.

Figure 6 relates regime duration to internal volatility. Short regimes (e.g., Period 13, 18 days) are not necessarily unstable; their internal volatility is actually low. In contrast, some long regimes (e.g., Period 5, 56 days) display high internal volatility, suggesting they contain unobserved sub-states. This validates the procedure's capacity to detect "short but intense" market episodes.

4.2. Deep-Dive into Four Extreme Regimes

Four extreme regimes are selected for in-depth case analysis (**Figure 7**). These states do not occur randomly; rather, they exhibit high synchronization with major macroeconomic and policy events.

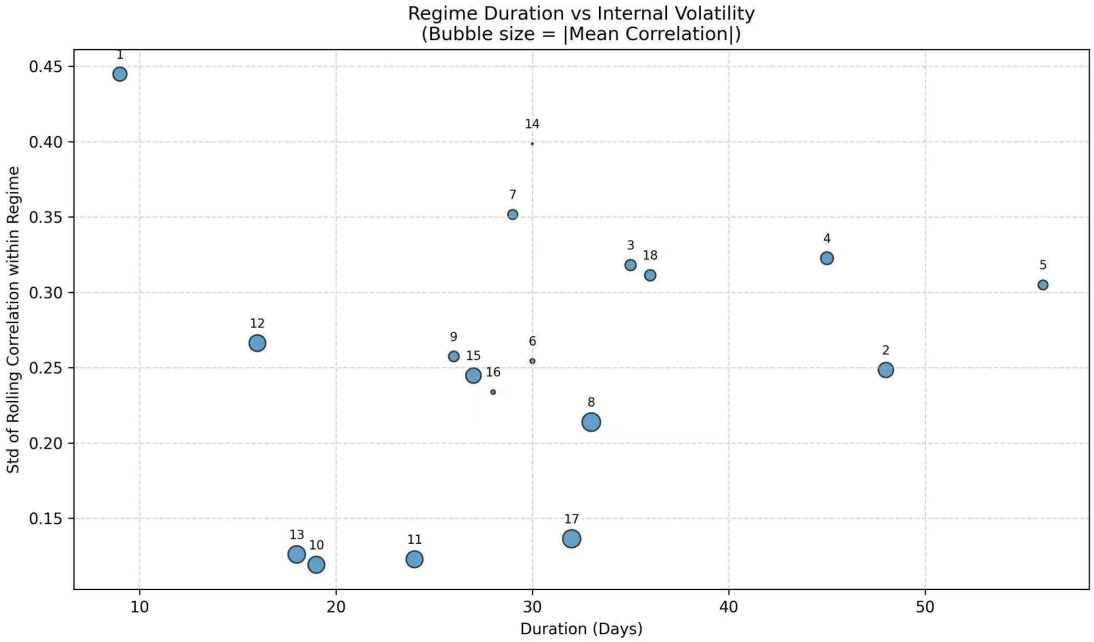

Figure 6. Regime duration vs internal volatility.

1) Period 8 (16 January-8 March 2024). This period exhibits the most negative rolling correlation (μ = −0.703, s.d. = 0.08). Margin-call rumors regarding snowball knock-in products (22 January) pushed the 5-day correlation to −0.862. Weaker holiday consumption data and a 15% month-over-month decline in new-home sales extended the bear-steepened to −0.917 by 5 February. The Two Sessions (4 March) confirmed an "around 5%" growth target without mega-stimulus, driving the correlation to −0.950 by 3 March. The IV Spread and index moved in lockstep negative territory, underscoring a "short-gamma, long-fear" regime.

2) Period 13 (16 July-8 August 2024). This 18-day window shows the strongest positive correlation (μ = 0.622, s.d. = 0.05). On 15 July, the PBoC cut the 1-year LPR by 10 basis points; on 31 July, exchanges released draft Implementation Rules for Programmed Trading; and on 8 August, the CSRC pledged to curb high-frequency volatility. Each announcement coincided with a monotonic rise in the 5-day correlation from 0.650 to 0.787, confirming that rate adjustments combined with regulatory guidance can shift the spread into a high-conviction buy signal regime.

3) Period 17 (17 December 2024-3 February 2025). This 32-day segment displays stable negative co-movement (μ = −0.675, s.d. = 0.068). On 16 December, the PBoC injected CNY 800 billion through 1-year MLF at 2.50% (−5 bp); on 20 December, China Securities Finance Corporation cut the broker refinancing rate by 30 basis points (CSF Notice 120); and on 27 December, DeepSeek released v3.0-Base (235B parameters), driving the CSI 300 technology sub-index up 1.2%. The 5-day correlation increased from 0.650 to 0.787 while the IV Spread narrowed 1.1 percentage points, indicating that modest policy easing and positive technology shocks generate low-noise momentum through the IV spre.

4) Period 5 (28 July -23 October 2023). This 56-day corridor records the widest intra-regime dispersion (μ = −0.191, s.d. = 0.22). On 9 June, convertible-bond trading collars took effect, pushing the 5-day correlation to −0.71; on 4 August, CSD&C cut the settlement reserve ratio to 13%, releasing an estimated CNY 30 billion of liquidity and lifting the correlation to −0.05; on 28 August, the Ministry of Finance halved the stamp duty to 0.05% and the CSRC bundled IPO tapering, lower margin ratios, and tighter short-selling surveillance, igniting a 3.5% single-day jump and flipping the correlation to +0.68. This sequence underscores how successive policy adjustments maintain the IV Spread in a policy-driven oscillation mode.

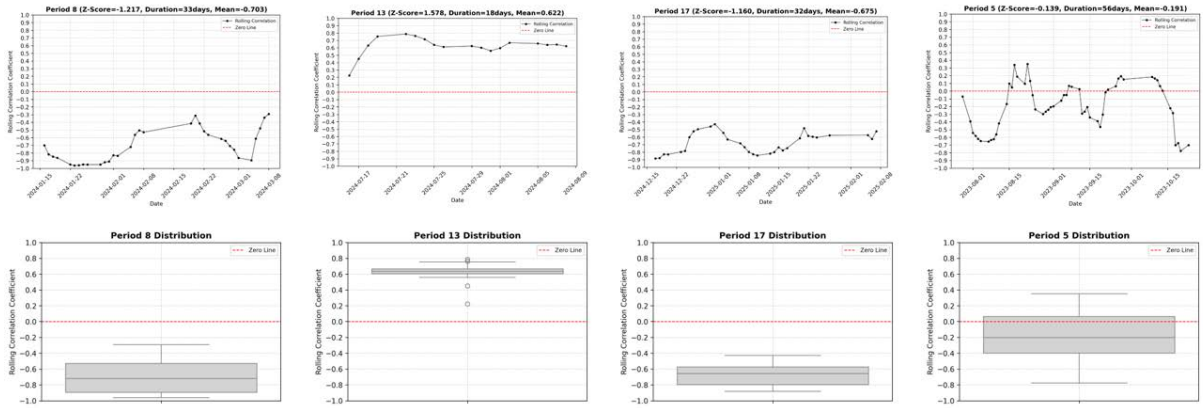

Figure 7. Time Series and Distribution of ρt (Period 8, 13, 17, 5).

4.3. Summary of Experimental Findings

Our empirical analysis reveals a dynamic, structurally unstable relationship between IV Spreads and CSI 300 ETF price movements. The two-stage change-point detection framework identifies 18 distinct regimes with correlations ranging from −0.703 to 0.622, confirming frequent shifts driven by macroeconomic conditions and policy interventions. The retention of shorter regimes (e.g., Periods 10, 12, 13) enables precise capture of "short but intense" market episodes.

Extreme correlation states synchronize with major policy events. Period 8 demonstrates that negative extremes coincide with deleveraging shocks, while Period 13 shows positive extremes aligning with monetary easing and regulatory guidance. This validates IV Spreads as real-time sentiment barometers, encoding both fear-driven hedging and speculation-driven momentum.

Regime differences carry critical implications for trading signals. High-conviction regimes—characterized by stable, extreme correlations—offer more reliable predictive power than transitional phases. The contrast between Period 5 (high internal volatility) and Period 13 (low internal volatility) underscores the necessity of regime-specific signal filtering.

These findings establish IV Spreads as a robust regime-switching indicator in the Chinese A-share market, providing a foundation for enhanced market timing

and risk management.

5. Conclusion

This study develops a dynamic correlation modeling and regime identification framework utilizing IV Spreads in the CSI 300 ETF options market. By analyzing the time-varying relationship between IV Spreads and underlying asset prices, we validate the indicator's effectiveness in forecasting market sentiment and price movements. Our key findings are as follows.

First, the IV Spread exhibits stronger and more consistent correlation with underlying asset movements than single-contract implied volatilities. In the Chinese market, the IV Spread captures not only directional expectations but also the dynamic equilibrium between speculative and hedging demands. Unlike mature markets, China's A-share options frequently exhibit inverted IV Spreads (call IV exceeding put IV), a phenomenon attributable to retail investor dominance, speculative trading culture, and limited short-selling mechanisms.

Second, rolling correlation analysis combined with change-point detection identifies multiple statistically stable market regimes, with correlations switching frequently among positive, negative, and neutral states. Notably, extreme correlation states synchronize closely with major macroeconomic policy events, indicating that IV Spreads effectively capture dynamic adjustments in risk perception following exogenous shocks. This confirms that IV Spreads contain structural information regarding how policy expectations and liquidity conditions reshape price dynamics.

Third, while this study focuses on quantitative IV Spread dynamics, incorporating unstructured data—such as news sentiment or search indices—could further enhance trading signal confidence. As IV Spreads already function as risk-sentiment proxies, integrating external sentiment measures would strengthen predictive power, particularly for early detection of regime shifts driven by policy or liquidity shocks.

This study has several limitations. First, the post-pandemic sample period has not yet experienced a complete bull-bear market cycle; the conclusion requires verification over extended time horizons. Second, the regime identification framework relies on empirical parameter thresholds; future research could employ machine learning methods for adaptive optimization. Third, the model's robustness to exogenous variables such as market liquidity and policy shocks warrants further examination.

Future research directions include: extending this framework to alternative asset classes (e.g., commodity options, foreign exchange options); integrating unstructured data sources to enhance sentiment recognition; and exploring IV Spread applications in portfolio risk management and strategic asset allocation.

Acknowledgements

We deeply appreciate the funding from the Basic and Applied Basic Research

Foundation of Guangdong Province (Project No. 2023B1515130002) and Shenzhen Science and Technology Plan Project (Shenzhen-Hong Kong-Macau Category C, No. SGDX20220530111001003) to make this research possible.

Conflicts of Interest

The authors declare no conflicts of interest regarding the publication of this paper.

References

Aminikhanghahi, S., & Cook, D. J. (2017). A Survey of Methods for Time Series Change Point Detection. *Knowledge and Information Systems, 51,* 339-367. https://doi.org/10.1007/s10115-016-0987-z

Andersen, T. G., Bollerslev, T., Diebold, F. X., & Labys, P. (2003). Modeling and Forecasting Realized Volatility. *Econometrica, 71,* 579-625. https://doi.org/10.1111/1468-0262.00418

Bakshi, G., & Kapadia, N. (2003). Delta-Hedged Gains and the Negative Market Volatility Risk Premium. *Review of Financial Studies, 16,* 527-566. https://doi.org/10.1093/rfs/hhg002

Beckers, S. (1981). Standard Deviations Implied in Option Prices as Predictors of Future Stock Price Variability. *Journal of Banking & Finance, 5,* 363-381. https://doi.org/10.1016/0378-4266(81)90032-7

Bing, T., & Ma, H. (2021). COVID-19 Pandemic Effect on Trading and Returns: Evidence from the Chinese Stock Market. *Economic Analysis and Policy, 71,* 384-396. https://doi.org/10.1016/j.eap.2021.05.012

Black, F., & Scholes, M. (1973). The Pricing of Options and Corporate Liabilities. *Journal of Political Economy, 81,* 637-654. https://doi.org/10.1086/260062

Blitz, D., Hanauer, M. X., & van Vliet, P. (2021). The Volatility Effect in China. *Journal of Asset Management, 22,* 338-349. https://doi.org/10.1057/s41260-021-00218-0

Bollen, N. P. B., & Whaley, R. E. (2004). Does Net Buying Pressure Affect the Shape of Implied Volatility Functions? *The Journal of Finance, 59,* 711-753. https://doi.org/10.1111/j.1540-6261.2004.00647.x

Bollerslev, T., & Zhou, H. (2002). Estimating Stochastic Volatility Diffusion Using Conditional Moments of Integrated Volatility. *Journal of Econometrics, 109,* 33-65. https://doi.org/10.1016/s0304-4076(01)00141-5

Bollerslev, T., Tauchen, G., & Zhou, H. (2009). Expected Stock Returns and Variance Risk Premia. *Review of Financial Studies, 22,* 4463-4492. https://doi.org/10.1093/rfs/hhp008

Chan, K., Menkveld, A. J., & Yang, Z. (2008). Information Asymmetry and Asset Prices: Evidence from the China Foreign Share Discount. *The Journal of Finance, 63,* 159-196. https://doi.org/10.1111/j.1540-6261.2008.01313.x

Chen, Y., & Lai, K. K. (2013). Examination on the Relationship between VHSI, HSI and Future Realized Volatility with Kalman Filter. *Eurasian Business Review, 3,* 200-216. https://doi.org/10.14208/ebr.2013.03.02.005

Chicago Board Options Exchange (1993). *The CBOE Volatility Index (VIX) [White Paper].* CBOE. https://www.cboe.com/tradable_products/vix/

DeMiguel, V., Plyakha, Y., Uppal, R., & Vilkov, G. (2013). Improving Portfolio Selection Using Option-Implied Volatility and Skewness. *Journal of Financial and Quantitative Analysis, 48,* 1813-1845. https://doi.org/10.1017/s0022109013000616

Derman, E., & Kani, I. (1994). *The Volatility Smile and Its Implied Tree [Goldman Sachs Quantitative Strategies Research Notes].* Goldman Sachs.

Derman, E., Kani, I., & Chriss, N. (1996). Implied Trinomial Tress of the Volatility Smile. *The Journal of Derivatives, 3,* 7-22. https://doi.org/10.3905/jod.1996.407952

Doran, J. S., Fodor, A., & Jiang, D. (2013). Call-Put Implied Volatility Spreads and Option Returns. *Review of Asset Pricing Studies, 3,* 258-290. https://doi.org/10.1093/rapstu/rat006

Du, J., Huang, D., Liu, Y., Shi, Y., Subrahmanyam, A., & Zhang, H. (2022). *Retail Investors and Momentum [Working Paper].* SSRN Working Paper No. 4163257. https://doi.org/10.2139/ssrn.4163257

Dupire, B. (1994). Pricing with a Smile. *Risk, 7,* 18-20.

Fung, J. K. W., Lam, F. Y. E., & Tse, Y. (2024). The Impact of ESG Rating on Hedging Downside Risks: Evidence from a Weight-Tilted Hang Seng Index. *Journal of Risk and Financial Management, 17,* Article No. 57. https://doi.org/10.3390/jrfm17020057

Goyal, A., & Saretto, A. (2009). Cross-Section of Option Returns and Volatility. *Journal of Financial Economics, 94,* 310-326. https://doi.org/10.1016/j.jfineco.2009.01.001

Guo, G., Qi, Y., Lai, S., Liu, Z., & Yen, J. (2023). The Latency Accuracy Trade-Off and Optimization in Implied Volatility-Based Trading Systems. *Expert Systems with Applications, 221,* Article ID: 119714. https://doi.org/10.1016/j.eswa.2023.119714

Hagan, P. S., Kumar, D., Lesniewski, A., & Woodward, D. (2002). Managing Smile Risk. *The Best of Wilmott, 1,* 249-296.

Heston, S. L. (1993). A Closed-Form Solution for Options with Stochastic Volatility with Applications to Bond and Currency Options. *Review of Financial Studies, 6,* 327-343. https://doi.org/10.1093/rfs/6.2.327

Hull, J., & White, A. (1987). The Pricing of Options on Assets with Stochastic Volatilities. *The Journal of Finance, 42,* 281-300. https://doi.org/10.1111/j.1540-6261.1987.tb02568.x

Johnson, T. L. (2017). Risk Premia and the VIX Term Structure. *Journal of Financial and Quantitative Analysis, 52,* 2461-2490. https://doi.org/10.1017/s0022109017000825

Keogh, E., Chu, S., Hart, D., & Pazzani, M. (2001). An Online Algorithm for Segmenting Time Series. In *Proceedings 2001 IEEE International Conference on Data Mining* (pp. 289-296). IEEE Computer Society. https://doi.org/10.1109/icdm.2001.989531

Lavielle, M. (2005). Using Penalized Contrasts for the Change-Point Problem. *Signal Processing, 85,* 1501-1510. https://doi.org/10.1016/j.sigpro.2005.01.012

Lin, T.-C., & Lu, X. (2015). Why Do Options Prices Predict Stock Returns? Evidence from Analyst Tipping. *Journal of Banking & Finance, 52,* 17-28. https://doi.org/10.1016/j.jbankfin.2014.11.008

Press, W. H., Teukolsky, S. A., Vetterling, W. T., & Flannery, B. P. (1992). *Numerical Recipes in C: The Art of Scientific Computing* (2nd ed.). Cambridge University Press.

Ross, S. A. (1976). The Arbitrage Theory of Capital Asset Pricing. *Journal of Economic Theory, 13,* 341-360. https://doi.org/10.1016/0022-0531(76)90046-6

Rubinstein, M. (1994). Implied Binomial Trees. *The Journal of Finance, 49,* 771-818. https://doi.org/10.1111/j.1540-6261.1994.tb00079.x

Smales, L. A. (2014). News Sentiment and the Investor Fear Gauge. *Finance Research Letters, 11,* 122-130. https://doi.org/10.1016/j.frl.2013.07.003

Whaley, R. E. (2000). The Investor Fear Gauge. *The Journal of Portfolio Management, 26,* 12-17. https://doi.org/10.3905/jpm.2000.319728

Xing, Y., Zhang, X., & Zhao, R. (2010). What Does the Individual Option Volatility Smirk Tell Us about Future Equity Returns? *Journal of Financial and Quantitative Analysis, 45,* 641-662. https://doi.org/10.1017/s0022109010000220

Yue, T., Zhang, J. E., & Tan, E. K. M. (2020). The Chinese Equity Index Options Market. *Emerging Markets Review, 45,* Article ID: 100742. https://doi.org/10.1016/j.ememar.2020.100742

Zhang, C., & Zi, C. (2025). *Understanding the Evolution of Momentum Effects in China's Stock Market [Working Paper].* https://czi.finance/assets/ChinaMom.pdf

Zhang, J. E., & Xiang, Y. (2008). The Implied Volatility Smirk. *Quantitative Finance, 8,* 263-284. https://doi.org/10.1080/14697680601173444